Journal of Zhejiang University SCIENCE A
ISSN 1673-565X (Print); ISSN 1862-1775 (Online)
www.zju.edu.cn/jzus; www.springerlink.com
E-mail: jzus@zju.edu.cn

Performance of the geometric approach to fault detection and isolation in SISO, MISO, SIMO and MIMO systems

RAHIMI N.[†1], SADEGHI M. H.[1], MAHJOOB M. J.[2]

([1]Mechanical Engineering Department, University of Tabriz, Tabriz 5166614766, Iran)

([2]Mechanical Engineering Department, University of Tehran, Tehran 1439957113, Iran)

[†]E-mail: nrahimi@ihu.ac.ir

Received Feb. 13, 2007; revision accepted June 17, 2007

Abstract: In this paper, a geometric approach to fault detection and isolation (FDI) is applied to a Multiple-Input Multiple-Output (MIMO) model of a frame and the FDI results are compared to the ones obtained in the Single-Input Single-Output (SISO), Multiple-Input Single-Output (MISO), and Single-Input Multiple-Output (SIMO) cases. A proper distance function based on parameters obtained from parametric system identification method is used in the geometric approach. ARX (Auto Regressive with eXogenous input) and VARX (Vector ARX) models with 12 parameters are used in all of the above-mentioned models. The obtained results reveal that by increasing the number of inputs, the classification errors reduce, even in the case of applying only one of the inputs in the computations. Furthermore, increasing the number of measured outputs in the FDI scheme results in decreasing classification errors. Also, it is shown that by using probabilistic space in the distance function, fault diagnosis scheme has better performance in comparison with the deterministic one.

Key words: Fault detection and isolation (FDI), Multivariate systems, Parametric system identification, Linear regression, Distance functions

doi:10.1631/jzus.2007.A1443 **Document code:** A **CLC number:** TB114.3; O224; O211.6

INTRODUCTION

Fault diagnosis methods are generally classified into two categories: system-based and model-based methods.

System-based methods consist mainly of hardware redundancy (voting) (Gilmore and McKern, 1970; Broan, 1974), software redundancy (Zimmerman and Lyde, 1993; Tokatli *et al.*, 2005) and fault-sensitive-filter (Hamelin *et al.*, 1999; De Persis and Isidori, 2001; Szaszi *et al.*, 2002; Frisk and Aslund, 2005) methods. Despite being used easily, system-based methods have major limitations and drawbacks namely: (1) requiring detailed mathematical models (usually in the state space form) of the process, (2) being suitable for sensor and actuator fault detection, but not, in general, applicable for system faults, and (3) being suitable for the deterministic case but suboptimal in the presence of the noise (Park, 1991; Willsky, 1976).

Model-based methods consist mainly of multiple model (Basseville *et al.*, 1986; Boukhris *et al.*, 2001), parametric modeling (Isermann, 1993; Bachschmid *et al.*, 2002) and Nearest Neighbor (Gersch *et al.*, 1983) methods. Those methods do not have the limitations and drawbacks of system-based methods, but their major drawback is that they fail if the operational mode is not exactly the same as any of the pre-modeled modes (Sadeghi and Fassois, 1991).

The geometric approach is a model-based method defined by using parametric models and distance functions and does not have the mentioned limitation where any fault is modeled by a hyper-plane; isolation of faults from the same category but with different magnitudes is possible (Sadeghi and Fassois, 1997). In most engineering applications, the parametric model-based fault diagnosis methods are based on the Single-Input Single-Output measurements (SISO or univariate models), and acceptable results are obtained (Sohn *et al*., 2003). However, there are cases where SISO model may not be appropriate for fault detection and isolation (FDI), and more accurate results are sought, wherein multivariate models may be the only alternative.

This approach has so far been used for fault isolation in univariate systems (Sakellariou and Fassois, 2000). In this study, the geometric approach to FDI has been extended to the multivariate systems and the results are compared with the ones obtained from the univariate cases. The system is a finite element model of a frame, with single or double force-acceleration (input-output) measurements. All of the models are considered linear and time-invariant systems with a single-fault at a time.

The modeling and FDI are explained in future sections. Then results and discussion are summarized, and the conclusion is given in the final section.

MODELING

In the geometric approach to FDI, an appropriate parametric model is selected for the system, and by using parametric system identification techniques, model parameters are obtained in any states. Then, any of no-fault and faulty mode model's parameters are represented as feature vectors, each being as a point in appropriate hyper-space. The feature vectors (or the points in the appropriate hyper-space) corresponding to the same modes are then approximated as hyper-planes, each of which representing a specific mode. The procedure applied to the considered frame is as follows.

Forming feature vector

The finite element model of the frame is shown in Fig.1. As shown in the figure, the frame has 10 elements and 4 supports. $\boldsymbol{F}_1$ and $\boldsymbol{F}_2$ are the input forces, while $\boldsymbol{a}_1$ and $\boldsymbol{a}_2$ are output accelerations (responses) of the system.

By running the finite element model for 100 s, 1000 sets of input-output data were recorded; 660 sets (corresponding to the seconds 2 to 67) were used for parametric modeling, and 330 sets (corresponding to the seconds 68 to 100) were used for validating step. Consequently, by applying 330 sets of unused data in

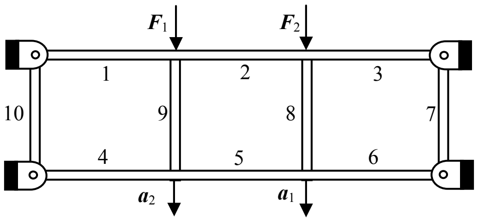

Fig.1 Schematic diagram of the frame

parameters estimation, validation was performed. This frame was modeled by the ARX (Auto Regressive with eXogenous input) and VARX (Vector ARX) models in the form of SISO, MISO (Multiple-Input Single-Output), SIMO (Single-Input Multiple-Output) and MIMO (Multiple-Input Multiple-Output) systems, respectively, as follows (Soderstrom and Stoica, 1989). The orders of the VARX and ARX models were selected within different orders by comparison of the models frequency and time-domain responses.

$$\sum_{na=0}^{4} a_{na} y(t-na) = \sum_{nb=0}^{3} b_{nb} u(t-nb) + w(t), \quad a_0 = 1, \tag{1}$$

$$\sum_{na=0}^{8} a_{na} y(t-na) = \begin{bmatrix} b_1 + b_2 q^{-1} & b_3 + b_4 q^{-1} \end{bmatrix} \begin{bmatrix} u_1(t) \\ u_2(t) \end{bmatrix} + w(t); \quad a_0 = 1, \tag{2}$$

$$\begin{bmatrix} 1 + a_1 q^{-1} + a_2 q^{-2} + a_3 q^{-3} & 0 \\ a_4 q^{-1} + a_5 q^{-2} & 1 + a_6 q^{-1} + a_7 q^{-2} + a_8 q^{-3} \end{bmatrix} \begin{bmatrix} y_1(t) \\ y_2(t) \end{bmatrix} = \begin{bmatrix} b_1 + b_2 q^{-1} \\ b_3 + b_4 q^{-1} \end{bmatrix} u(t) + \begin{bmatrix} w_1(t) \\ w_2(t) \end{bmatrix}, \tag{3}$$

$$\begin{bmatrix} 1 + a_1 q^{-1} + a_2 q^{-2} + a_3 q^{-3} & 0 \\ a_4 q^{-1} + a_5 q^{-2} & 1 + a_6 q^{-1} + a_7 q^{-2} + a_8 q^{-3} \end{bmatrix} \begin{bmatrix} y_1(t) \\ y_2(t) \end{bmatrix} = \begin{bmatrix} b_1 & b_2 \\ b_3 & b_4 \end{bmatrix} \begin{bmatrix} u_1(t) \\ u_2(t) \end{bmatrix} + \begin{bmatrix} w_1(t) \\ w_2(t) \end{bmatrix}, \tag{4}$$

where y, u and w are output, input and noise signals, respectively. Also, a and b are coefficients and q^{-1} is the backshift as follows:

$$q^{-1} y(t) = y(t-1).$$

The first canonical form of the parametric models is used in VARX models. The general form of VARX model is:

$$\boldsymbol{A}(q^{-1})\boldsymbol{Y}(t) = \boldsymbol{B}(q^{-1})\boldsymbol{U}(t-k) + \boldsymbol{W}(t),$$

where $\boldsymbol{A}(q^{-1})$ and $\boldsymbol{B}(q^{-1})$ are matrix polynomials where $\boldsymbol{A}(q^{-1})$ in double-output models is as follows:

$$\boldsymbol{A}(q^{-1})=\begin{bmatrix} A_1(q^{-1}) & A_2(q^{-1}) \\ A_3(q^{-1}) & A_4(q^{-1}) \end{bmatrix}.$$

The first canonical form is defined such that the matrix polynomial $\boldsymbol{A}(q^{-1})$ obeys the following conditions (Kashyap and Rao, 1976):

(1) $\boldsymbol{A}(q^{-1})$ is lower triangular (i.e., $A_2(q^{-1})=0$ in our model);

(2) $\boldsymbol{A}(0)=\boldsymbol{I}$; thus in our model:

$$\begin{aligned} A_1(q^{-1}) &= 1+a_{11}q^{-1}+a_{12}q^{-2}+\cdots+a_{1l}q^{-l}, \\ A_3(q^{-1}) &= a_{31}q^{-1}+a_{32}q^{-2}+\cdots+a_{3g}q^{-g}, \\ A_4(q^{-1}) &= 1+a_{41}q^{-1}+a_{42}q^{-2}+\cdots+a_{4r}q^{-r}. \end{aligned}$$

(3) degree of $A_3(q^{-1})\leq$degree of $A_4(q^{-1})$ (i.e., $g\leq r$);

(4) $\boldsymbol{B}(q^{-1})$ is arbitrary.

All the above-mentioned models are written in the following linear regression form:

$$\boldsymbol{Y}(t)=\boldsymbol{\Phi}^{\mathrm{T}}(t)\boldsymbol{\theta}+\boldsymbol{W}(t), \tag{5}$$

where $\boldsymbol{Y}(t)$ and $\boldsymbol{W}(t)$ are the output and noise signals, respectively; in single-output and two-output models, they are:

$$\boldsymbol{W}(t)=w(t), \quad \boldsymbol{Y}(t)=y(t);$$

$$\boldsymbol{W}(t)=\begin{bmatrix} w_1(t) \\ w_2(t) \end{bmatrix}, \quad \boldsymbol{Y}(t)=\begin{bmatrix} y_1(t) \\ y_2(t) \end{bmatrix}.$$

The inputs and outputs of the models are chosen to be:

$$\text{MIMO}:\begin{cases} u_1=|\boldsymbol{F}_1|, u_2=|\boldsymbol{F}_2|; \\ y_1=|\boldsymbol{a}_1|, y_2=|\boldsymbol{a}_2|, \end{cases} \quad \text{MISO}:\begin{cases} u_1=|\boldsymbol{F}_1|, u_2=|\boldsymbol{F}_2|; \\ y=|\boldsymbol{a}_1|, \end{cases}$$

$$\text{SIMO}:\begin{cases} u=|\boldsymbol{F}_1|; \\ y_1=|\boldsymbol{a}_1|, y_2=|\boldsymbol{a}_2|, \end{cases} \quad \text{SISO}:\begin{cases} u=|\boldsymbol{F}_1|; \\ y=|\boldsymbol{a}_1|. \end{cases}$$

$\boldsymbol{\Phi}(t)$ which include any type of the above models are selected to be:

$$\boldsymbol{\Phi}(t)_{\text{SISO}}=\begin{bmatrix} y(t-1) \\ y(t-2) \\ y(t-3) \\ y(t-4) \\ y(t-5) \\ y(t-6) \\ y(t-7) \\ y(t-8) \\ u(t) \\ u(t-1) \\ u(t-2) \\ u(t-3) \end{bmatrix}, \boldsymbol{\Phi}(t)_{\text{SIMO}}=\begin{bmatrix} y_1(t-1) & 0 \\ y_1(t-2) & 0 \\ y_1(t-3) & 0 \\ u(t) & 0 \\ u(t-1) & 0 \\ 0 & y_1(t-1) \\ 0 & y_1(t-2) \\ 0 & y_2(t-1) \\ 0 & y_2(t-2) \\ 0 & y_2(t-3) \\ 0 & u(t) \\ 0 & u(t-1) \end{bmatrix},$$

$$\boldsymbol{\Phi}(t)_{\text{MISO}}=\begin{bmatrix} y(t-1) \\ y(t-2) \\ y(t-3) \\ y(t-4) \\ y(t-5) \\ y(t-6) \\ y(t-7) \\ y(t-8) \\ u_1(t) \\ u_1(t-1) \\ u_2(t) \\ u_2(t-1) \end{bmatrix}, \boldsymbol{\Phi}(t)_{\text{MIMO}}=\begin{bmatrix} y_1(t-1) & 0 \\ y_1(t-2) & 0 \\ y_1(t-3) & 0 \\ u_1(t) & 0 \\ u_2(t) & 0 \\ 0 & y_1(t-1) \\ 0 & y_1(t-2) \\ 0 & y_2(t-1) \\ 0 & y_2(t-2) \\ 0 & y_2(t-3) \\ 0 & u_1(t) \\ 0 & u_2(t) \end{bmatrix}.$$

The parametric feature vector in all of the above mentioned models is:

$$\boldsymbol{\theta}=[\theta_1 \ \theta_2 \ \theta_3 \ \theta_4 \ \theta_5 \ \theta_6 \ \theta_7 \ \theta_8 \ \theta_9 \ \theta_{10} \ \theta_{11} \ \theta_{12}]^{\mathrm{T}},$$

which consists of 12 entities (eight of which are corresponding to the autoregressive estimated parameters, and the remaining four are associated with the exogenous ones). By casting the obtained data from the finite element model in the linear regression form, the following set of equations are obtained:

$$\begin{cases} \boldsymbol{Y}(1)=\boldsymbol{\Phi}^{\mathrm{T}}(1)\boldsymbol{\theta}+\boldsymbol{W}(1), \\ \boldsymbol{Y}(2)=\boldsymbol{\Phi}^{\mathrm{T}}(2)\boldsymbol{\theta}+\boldsymbol{W}(2), \\ \ldots, \\ \boldsymbol{Y}(N)=\boldsymbol{\Phi}^{\mathrm{T}}(N)\boldsymbol{\theta}+\boldsymbol{W}(N), \end{cases}$$

$$\Rightarrow \begin{bmatrix} \boldsymbol{Y}(1) \\ \boldsymbol{Y}(2) \\ \vdots \\ \boldsymbol{Y}(N) \end{bmatrix} = \begin{bmatrix} \boldsymbol{\Phi}^{\mathrm{T}}(1) \\ \boldsymbol{\Phi}^{\mathrm{T}}(2) \\ \vdots \\ \boldsymbol{\Phi}^{\mathrm{T}}(N) \end{bmatrix} \begin{bmatrix} \theta_1 \\ \theta_2 \\ \vdots \\ \theta_{12} \end{bmatrix} + \begin{bmatrix} \boldsymbol{W}(1) \\ \boldsymbol{W}(2) \\ \vdots \\ \boldsymbol{W}(N) \end{bmatrix}, \quad (6)$$

where N is the number of measurements (or the number of input-output sets). The compact form of Eq.(6) may be written as:

$$\boldsymbol{Y}=\boldsymbol{\Phi\theta}+\boldsymbol{W}, \quad (7)$$

where the prediction error vector is:

$$\boldsymbol{W}= \boldsymbol{Y}-\boldsymbol{\Phi\theta}, \quad (8)$$

where $\boldsymbol{Y}$ and $\boldsymbol{\Phi}$ for one-output models are an $N\times1$ vector and an $N\times12$ matrix, and for two-output models are a $2N\times1$ vector, and a $2N\times12$ matrix, respectively. If the number of measurements in the one-output models is 12, $\boldsymbol{\Phi}$ will be a square matrix, and if $\boldsymbol{\Phi}$ is non-singular, the parameter vector will have a unique answer which is obtained from solving the set of linear Eq.(6). Due to the disturbances and model errors, more data will be used (i.e., $N>12$). Also, since the first and second rows of $\boldsymbol{\Phi}$ in the two-output models have 4 and 8 non-zero members, respectively, the number of measurements will be more than 8 times (i.e., $N>8$). Finally, the parameter vector $\boldsymbol{\theta}$ in any of SISO, MISO, SIMO, and MIMO models will be obtained by minimizing prediction errors and the least squares method in the following way (Soderstrom and Stoica, 1989):

$$\boldsymbol{\theta}=[\boldsymbol{\Phi}^{\mathrm{T}}\boldsymbol{\Phi}]^{-1}\boldsymbol{\Phi}^{\mathrm{T}}\,\boldsymbol{Y}. \quad (9)$$

The input and output signals selection were performed by considering the model limitation and comparison of the fault diagnosis results in different states to have the least error in fault diagnosis results.

The random input signals u_1 and u_2 with intensity of 5 and 3 units, respectively, are shown in Fig.2. For validation, the frequency response function (*FRF*) based on power spectrum estimation of the input-output signals obtained from the simulation is compared to the one obtained from the parametric modeling which is depicted in Fig.3. Also the simulation and one-step-ahead prediction results for SISO, MISO, SIMO, and MIMO models are shown in Figs.4 to 7. In Figs.3~7, grey and black lines mean finite element and parametric models, respectively.

Since the comparison of results corresponding to both probabilistic and deterministic spaces is considered in validation, the feature vector $\boldsymbol{\theta}$ and the distance function in the two mentioned spaces will be used as follows (Luenberger, 1986).

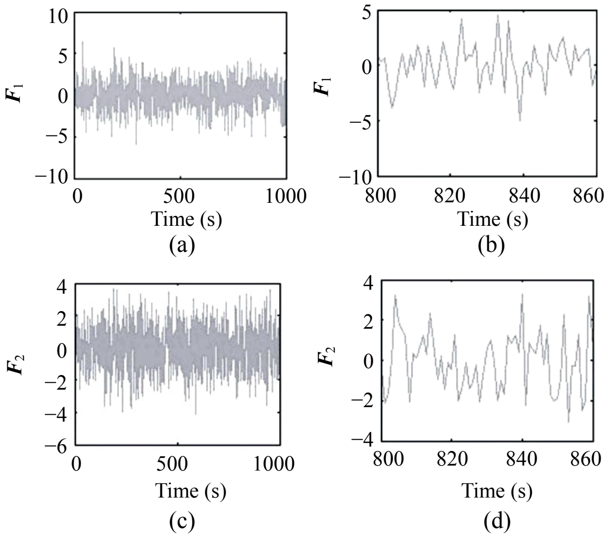

Fig.2 Input signals (the time scale is 0.1 s). (a) All data of first input; (b) Zoomed data of first input; (c) All data of second input; (d) Zoomed data of second input

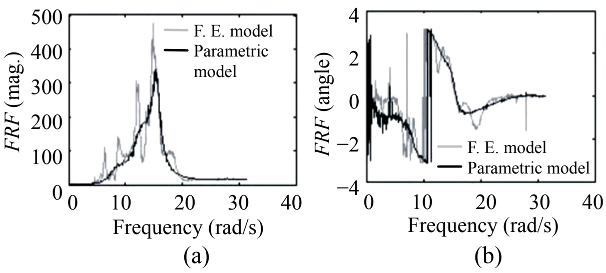

Fig.3 Frequency response of the SISO frame's finite element and parametric models. (a) Magnitude; (b) Phase angle

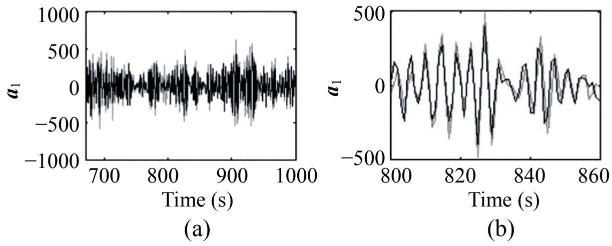

Fig.4 Single-Input Single-Output models' responses (the time scale is 0.1 s). (a) Validation data; (b) Zoomed for see details

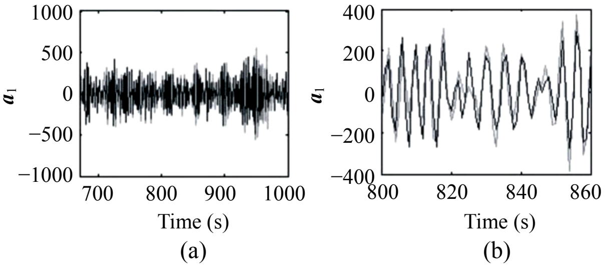

Fig.5 Two-Input Single-Output models' responses (the time scale is 0.1 s). (a) Validation data; (b) Zoomed for see details

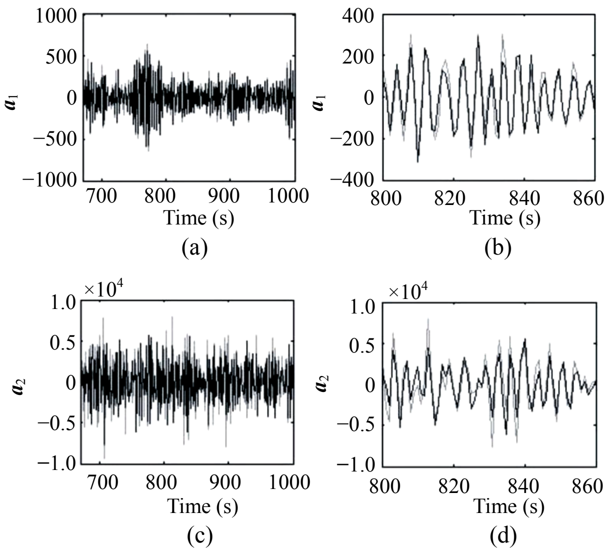

Fig.6 Single-Input Two-Output models' responses (the time scale is 0.1 s). (a) Validation data of first output; (b) Zoomed data of first output; (c) Validation data of second output; (d) Zoomed data of second output

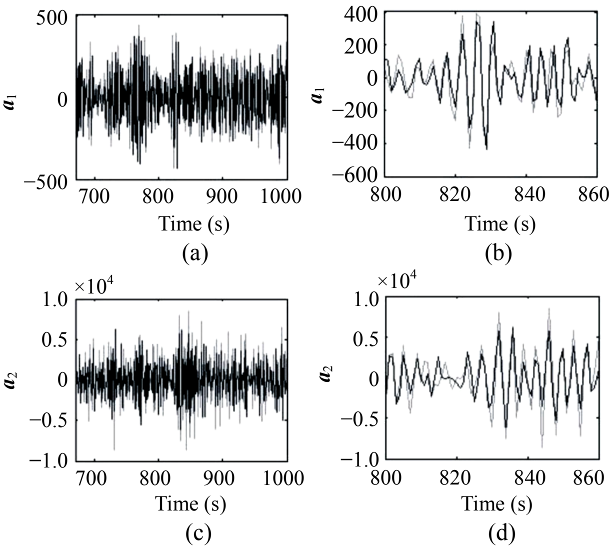

Fig.7 Two-Input Two-Output models' responses (the time scale is 0.1 s). (a) Validation data of first output; (b) Zoomed data of first output; (c) Validation data of second output; (d) Zoomed data of second output

In the deterministic space, the members of feature vector $\boldsymbol{\theta}$ include only the model's parameters, so, the feature vector $\boldsymbol{\theta}$ and the distance function of two vectors are as follows:

$$\boldsymbol{\theta} = [\boldsymbol{\mu}_{\boldsymbol{\theta}}]^{\mathrm{T}} = \begin{bmatrix} \theta_1 & \theta_2 & \dots & \theta_{12} \end{bmatrix}^{\mathrm{T}}, \tag{10}$$

$$D(\boldsymbol{\theta},\boldsymbol{\theta}^u) = \mathrm{tr}[(\boldsymbol{\mu}_{\boldsymbol{\theta}} - \boldsymbol{\mu}_{\boldsymbol{\theta}}^u)(\boldsymbol{\mu}_{\boldsymbol{\theta}} - \boldsymbol{\mu}_{\boldsymbol{\theta}}^u)^{\mathrm{T}}], \tag{11}$$

while in the probabilistic space, the members of feature vector $\boldsymbol{\theta}$ include the model's parameters as well as their variances. Therefore, in this space, the feature vector $\boldsymbol{\theta}$ and distance function of two vectors are:

$$\boldsymbol{\theta} = [\boldsymbol{\mu}_{\boldsymbol{\theta}} | (\mathrm{diag}\boldsymbol{P}_{\boldsymbol{\theta}})^{\mathrm{T}}]^{\mathrm{T}} = \begin{bmatrix} \theta_1, \cdots, \theta_{12} & \sigma_{\theta_1}^2, \cdots, \sigma_{\theta_{12}}^2 \end{bmatrix}^{\mathrm{T}}, \tag{12}$$

$$D(\boldsymbol{\theta},\boldsymbol{\theta}^u) = \mathrm{tr}[(\boldsymbol{\mu}_{\boldsymbol{\theta}} - \boldsymbol{\mu}_{\boldsymbol{\theta}}^u)(\boldsymbol{\mu}_{\boldsymbol{\theta}} - \boldsymbol{\mu}_{\boldsymbol{\theta}}^u)^{\mathrm{T}} + (\boldsymbol{\sigma}_{\boldsymbol{\theta}}^2 - \boldsymbol{\sigma}_{\boldsymbol{\theta}^u}^2)(\boldsymbol{\sigma}_{\boldsymbol{\theta}}^2 - \boldsymbol{\sigma}_{\boldsymbol{\theta}^u}^2)^{\mathrm{T}}]. \tag{13}$$

Parameters' variances, which are the diagonal members of the parameters' covariance matrix, are obtained as follows (Ljung, 1999):

$$\begin{aligned} &\boldsymbol{P}_{\boldsymbol{\theta}} := \mathrm{cov}(\boldsymbol{\theta}) = \lambda_0 (\boldsymbol{\Phi}^{\mathrm{T}} \boldsymbol{\Phi})^{-1}, \\ &\lambda_0 = \mathrm{mean}[(\boldsymbol{Y} - \boldsymbol{\Phi\theta})^{\mathrm{T}} (\boldsymbol{Y} - \boldsymbol{\Phi\theta})] / (N-12), \end{aligned} \tag{14}$$

Modeling of probable modes

Probable faulty modes (no-fault and faulty) are modeled in the form of reduction of stiffness caused by events like crack, cavity and impurity in any of the elements 1, 2, and 3. Considering the presence of inevitable non-homogeneity in the process of production parts, reduction of stiffness is allowed up to 5%, and the no-fault mode is modeled by creating such a state in any of the elements. The locus of feature vectors corresponding to ith mode (i=1,2,3,4) is a hyper-plane. In the deterministic space, the equation of the hyper-plane is:

$$\theta_1 + \theta_2 \alpha_1^i + \theta_3 \alpha_2^i + \cdots + \theta_{12} \alpha_{11}^i + \alpha_0^i = 0, \tag{15}$$

where α_j^i (j=0,1,2,…,11) are the hyper-plane's coefficients, that is, the normal vector $\boldsymbol{n}^i$, representing the ith hyper-plane is:

$$\boldsymbol{n}^i = [1 \;\; \alpha_1^i \;\; \alpha_2^i \;\; \cdots \;\; \alpha_{11}^i]^{\mathrm{T}}. \tag{16}$$

The set of equations to obtain the hyper-plane's coefficients will be:

$$f^i(\boldsymbol{\theta}) = (\boldsymbol{n}^i)^{\mathrm{T}}\boldsymbol{\theta} + \alpha_0^i = 0. \tag{17}$$

In order to estimate the coefficients of any mode's hyper-plane, that is the ith operational mode, the following procedures were carried out: a certain reduction of stiffness (or, elasticity module) was applied to a specific element and considered to be a state (a point on the representing hyper-plane), and the finite element model was run for each one of the 25 states or 49 states, in deterministic or probabilistic spaces, respectively. Since any of the feature vectors obtained from the above-mentioned states corresponding to the ith operational mode must satisfy the equation of the ith hyper-plane, the following set of equations in the deterministic space were obtained:

$$\begin{cases} \theta_1^{i1} + \theta_2^{i1}\alpha_1^i + \theta_3^{i1}\alpha_2^i + \cdots + \theta_{12}^{i1}\alpha_{11}^i + \alpha_0^i = 0, \\ \theta_1^{i2} + \theta_2^{i2}\alpha_1^i + \theta_3^{i2}\alpha_2^i + \cdots + \theta_{12}^{i2}\alpha_{11}^i + \alpha_0^i = 0, \\ \cdots, \\ \theta_1^{i25} + \theta_2^{i25}\alpha_1^i + \theta_3^{i25}\alpha_2^i + \cdots + \theta_{12}^{i25}\alpha_{11}^i + \alpha_0^i = 0. \end{cases} \tag{18}$$

In the probabilistic space, 49 equations were obtained in similar way. To estimate the hyper-plane's coefficients, the above-mentioned set of equations is in the form of linear regression as:

$$\begin{bmatrix} 1 & \theta_2^{i1} & \theta_3^{i1} & \cdots & \theta_{12}^{i1} \\ 1 & \theta_2^{i2} & \theta_3^{i2} & \cdots & \theta_{12}^{i2} \\ \vdots & \vdots & \vdots & & \vdots \\ 1 & \theta_2^{i25} & \theta_3^{i25} & \cdots & \theta_{12}^{i25} \end{bmatrix} \begin{bmatrix} \alpha_0^i \\ \alpha_1^i \\ \vdots \\ \alpha_{11}^i \end{bmatrix} = -\begin{bmatrix} \theta_1^{i1} \\ \theta_1^{i2} \\ \vdots \\ \theta_1^{i25} \end{bmatrix}, \tag{19}$$

or in the compact form:

$$\boldsymbol{\psi}^i \boldsymbol{\alpha}^i = -\boldsymbol{a}_1^i, \tag{20}$$

where $\boldsymbol{\alpha}^i$ and $\boldsymbol{\psi}^i$ are a 12×1 vector and a 25×12 matrix, respectively. Taking into account the effect of noise and other (random) errors, the number of equations (i.e., the number of states) was selected to be more than two times that of the number of the hyper-plane's coefficients. The hyper-plane's coefficients were estimated by the least squares method as follows (Myers, 1990):

$$\boldsymbol{\alpha}^i = [(\boldsymbol{\psi}^i)^{\mathrm{T}}\boldsymbol{\psi}^i]^{-1}(\boldsymbol{\psi}^i)^{\mathrm{T}}(-\boldsymbol{a}_1^i). \tag{21}$$

FAULT DETECTION AND ISOLATION

The distances between the estimated feature vector of an operational mode (as a point on the hyper-space) and each of the hyper-planes are calculated; the operational mode is designated as that mode whose distance is minimal. Reduction of elasticity module (or, stiffness) in any of the elements 1, 2, and 3 to the amount of 1%, 2%, 3%, 4%, 10%, 20%, 30%, 40%, 50%, 60%, 70%, and 80% of the nominal value, was considered as operational (unknown) modes. FDI was performed in 37 operational states (13 of them were corresponding to the no-fault mode and the remaining 24 were associated with the faulty modes). These operational modes were not used in forming the hyper-planes. For FDI, the distance between feature vector of the unknown operational mode $\boldsymbol{\theta}^u$, and each of the hyper-planes represented by the normal vector $\boldsymbol{n}^i$, should be calculated. The distance calculation is based upon minimizing the distance between vector $\boldsymbol{\theta}^u$ and each of the hyper-planes (Luenberger, 1986). Since the distance function is always non-negative and monotonic, in order to increase the computational efficiency, the quadratic form of the distance function was minimized. To convert the constrained minimization to an unconstrained optimization, the Lagrange Multipliers approach was adopted (Strang, 1986). The Lagrangian is obtained as follows:

$$\begin{aligned} L &= d^2(\boldsymbol{\theta}^u, \boldsymbol{\theta}) + \gamma f^i(\boldsymbol{\theta}) \\ &= (\boldsymbol{\theta}^u - \boldsymbol{\theta})(\boldsymbol{\theta}^u - \boldsymbol{\theta})^{\mathrm{T}} + \gamma(\boldsymbol{n}^i\boldsymbol{\theta} + \alpha_0^i), \end{aligned} \tag{22}$$

where γ and $d(\boldsymbol{\theta}^u, \boldsymbol{\theta})$ are the Lagrange multiplier and the distance between vector $\boldsymbol{\theta}^u$ and vectors $\boldsymbol{\theta}$, respectively. The optimizing of L is equivalent to minimizing the distance function subject to $f^i(\boldsymbol{\theta})=0$. Differentiation of L with respect to $\boldsymbol{\theta}$ and γ leads to a set of 1+12 linear equations of the form:

$$\begin{bmatrix} \boldsymbol{I} & \boldsymbol{n}^i \\ (\boldsymbol{n}^i)^{\mathrm{T}} & \boldsymbol{0} \end{bmatrix} \begin{bmatrix} \boldsymbol{\theta} \\ \gamma \end{bmatrix} = \begin{bmatrix} \boldsymbol{\theta}^u \\ -\alpha_0^i \end{bmatrix}, \tag{23}$$

where $\boldsymbol{I}$ is a 12×12 identity matrix. Solving Eq.(23) results in the distance between vector $\boldsymbol{\theta}^u$ and $f^i(\boldsymbol{\theta})=0$ yielding:

$$d(\boldsymbol{\theta}^u, f^i(\boldsymbol{\theta}))=\min d(\boldsymbol{\theta}^u,\boldsymbol{\theta})=\boldsymbol{n}^i[(\boldsymbol{n}^i)^{\mathrm{T}}\boldsymbol{n}^i]^{-1}[(\boldsymbol{n}^i)^{\mathrm{T}}\boldsymbol{\theta}^u+\alpha_0^i],\quad \boldsymbol{\theta}\in f^i(\boldsymbol{\theta}). \tag{24}$$

By repeating the above-mentioned procedure for each one of the hyper-planes (operational modes), the distances between the vector $\boldsymbol{\theta}^u$ and the hyper-planes are obtained. Finally these calculated distances are compared with each other and the unknown operational mode is classified as the mode with which the calculated distance is the minimum. That is:

$$d(\boldsymbol{\theta}^u, f^i(\boldsymbol{\theta}))<d(\boldsymbol{\theta}^u, f^j(\boldsymbol{\theta})),\ \forall i\neq j;\ i,j=1,2,3,4,\quad \boldsymbol{\theta}^u\in f^i(\boldsymbol{\theta}). \tag{25}$$

RESULTS AND DISCUSSION

As mentioned earlier, in geometric approach, fault diagnosis is done through parametric system identification handling signals with random nature. Therefore, the results of fault diagnosis are obtained probabilistically, so, to evaluate and compare the FDI results of different models, the mean value and the variance of the number of classification errors in any of the models were used, via Mont-Carlo simulation. To this end, fault diagnosis scheme was performed 50 times for each of the models, then the mean and variance of classification errors in any of the models was obtained. The obtained results in the probabilistic and deterministic spaces by 49 and 25 states are presented in Table 1.

As can be observed from Table 1, using the probabilistic space has the highest performance among different types of the spaces; these results are shown in Fig.8.

The above results show that increasing the number of inputs improves the FDI performance; as classification error in MIMO model is less than SIMO one, and in MISO model is less than SISO one. The reason is the outputs' further enrichment, which is caused by further activation of the system dynamics caused by increasing the number of inputs. This concept is also true in the cases where two inputs are applied to the system, but one of them is used in computations. Also fault diagnosis scheme in two-output models performs better compared to single-output ones; as classification error in MIMO model is less than MISO one, and in SIMO model is less than SISO one. The reason is to acquire further information on the system dynamics through increasing the number of outputs. While the parametric system identification in two-output models can be done by using less measurement (N>8) than that in single-output models (N>12).

However, it should be mentioned that the effect of inputs number on FDI performance is more marked compared to the outputs one, as classification error in MISO model is less than that in SIMO model. The reason is that the increase in the number of inputs excites the system dynamics more effective, while by increasing the number of outputs, the obtained data from the system dynamics increase.

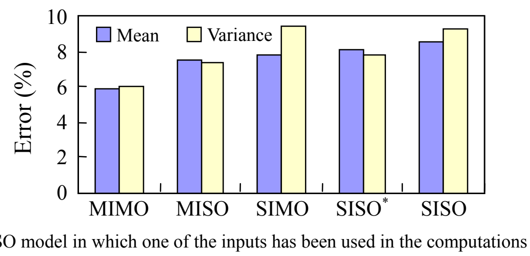

Fig.8 Classification errors in different models

Table 1 Classification errors (misclassifications) in 37 operational modes

	Probabilistic with 49 states		Deterministic with 49 states		Deterministic with 25 states	
	Mean value (and percent)	Variance value (and percent)	Mean value (and percent)	Variance value (and percent)	Mean value (and percent)	Variance value (and percent)
MIMO	2.15 (5.81%)	2.25 (6.08%)	2.75 (7.43%)	3.00 (8.11%)	3.15 (8.51%)	3.26 (8.81%)
MISO	2.78 (7.51%)	2.71 (7.32%)	11.00 (29.73%)	3.76 (10.16%)	11.32 (30.60%)	4.26 (11.51%)
SIMO	2.88 (7.78%)	3.46 (9.35%)	6.34 (17.14%)	9.62 (26.00%)	6.70 (18.11%)	10.79 (29.16%)
SISO*	3.00 (8.11%)	2.90 (7.84%)	9.40 (25.41%)	6.57 (17.76%)	10.06 (27.19%)	5.89 (15.92%)
SISO	3.14 (8.49%)	3.43 (9.27%)	9.44 (25.51%)	5.93 (16.03%)	10.54 (28.49%)	6.09 (16.46%)

* MISO model in which one of the inputs has been used in the computations

By using probabilistic space in calculation of distances and utilizing variances of the estimated parameters in addition to the parameters themselves, the FDI performance is noticeably improved in comparison to the deterministic one. Since the number of used parameters in the probabilistic distance function was almost twice that of the deterministic one, it may be thought that increasing the number parameters is the main cause of performance improvement. In order to investigate this, fault diagnosis based on deterministic space was performed by increasing the modeling mode numbers to 49 states and the FDI results were compared to that of probabilistic ones which are shown in Fig.9. As it is concluded from the figure, increasing the number of parameters from 25 to 49 in deterministic space improved the FDI performance slightly; the performance in probabilistic space is still much better than that of deterministic space.

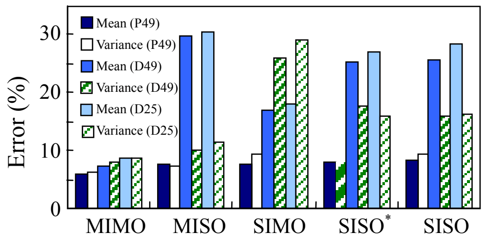

*MISO model in which one of the inputs has been used in the computations

Fig.9 Fault diagnosis errors in the probabilistic and deterministic spaces

CONCLUSION

In order to study the performance of geometric approach to FDI, fault diagnosis scheme was applied to the SISO, MISO, SIMO and MIMO models of the frame.

The results demonstrated that the increase in the number of inputs causes the decrease in classification errors, as the superior performances were associated with the models having two inputs (even applying only one of the inputs in the computations).

The increase in the number of the outputs, although less marked, also caused reduction in FDI errors, as FDI in the two-output models had less classification errors compared to the single-output models. In summary, the rank of the performance of the models was: MIMO, MISO, SIMO and SISO, respectively.

Finally, the performance of FDI in the probabilistic space was better than that in the deterministic space. While, the FDI accuracy of the MIMO model was the most in the deterministic space.

References

Bachschmid, N., Pennacchi, T., Venia, A., 2002. Identification of multiple faults in rotor systems. *Journal of Sound and Vibration*, **254**(2):327-366. [doi:10.1006/jsvi.2001.4116]

Basseville, M.A., Benveniste, A., Moustakides, G.V., Rougee, A., 1986. Detection and diagnosis of abrupt changes in modal characteristics of nonstationary digital signals. *IEEE Transaction on Information Theory*, **32**(3):412-417. [doi:10.1109/TIT.1986.1057180]

Boukhris, A., Giuliani, S., Mourot, G., 2001. Rainfall-runoff multi-modelling for sensor fault diagnosis. *Control Engineering Practice*, **9**(6):659-671. [doi:10.1016/S0967-0661(01)00022-3]

Broan, R.B., 1974. A Nonlinear Voter-estimator for Redundant Systems. Proceedings of IEEE Conf. on Decision and Control, Phoenix, AZ, p.743-748.

De Persis, C., Isidori, A., 2001. A geometric approach to nonlinear fault detection and isolation. *IEEE Transactions on Automatic Control*, **46**(6):853-865. [doi:10.1109/9.928586]

Frisk, E., Aslund, J., 2005. Lowering orders of derivatives in non-linear residual generation using realization theory. *Automatica*, **41**(10):1799-1807. [doi:10.1016/j.automatica.2005.04.022]

Gersch, W., Brotherton, T., Braun, S., 1983. Nearest neighbor time series analysis classification of faults in rotating machinery. *ASME Journal of Vibration, Acoustics, Stress, and Reliability in Design*, **105**:178-184.

Gilmore, J., McKern, R., 1970. A Redundant Strap-down Inertial Systems Mechanization. AIAA Guidance, Control, and Flight Mechanics Conf., Santa Barbara, CA, p.17-19.

Hamelin, F., Defranoux, C., Rambeaux, F., 1999. A Geometric Approach for Fault Detection and Isolation in Dynamic Uncertain Systems. Proceeding of 38th IEEE Conf. Decision and Control, Phoenix, Arizona, USA, **3**:3122-3127.

Isermann, R., 1993. Fault diagnosis of machines via parameter estimation and knowledge processing. *Automatica*, **29**(4):815-835. [doi:10.1016/0005-1098(93)90088-B]

Kashyap, R.L., Rao, A.R., 1976. Dynamic Stochastic Models from Empirical Data. Academic Press.

Ljung, L., 1999. System Identification Theory for the User (2nd Ed.). Prentice Hall.

Luenberger, D., 1986. Optimization by Vector Space Method. Wiley.

Myers, R.H., 1990. Classical and Modern Regression with Applications (2nd Ed.). Advanced Series in Statistics and Decision Science. Duxbury Press.

Park, J., 1991. A Unified Approach to Fault Detection and Isolation in Dynamical System. Ph.D Thesis, Department of Electrical Engineering and Computer Science, University of Michigan, Ann Arbor, MI.
Sadeghi, M.H., Fassois, S.D., 1991. A Stochastic Approach to the Failure Detection and Isolation Problem for Automobile Hydraulic Active Suspension System. Technical Report submitted to the Ford Motor Company, Dearborn, MI.
Sadeghi, M.H., Fassois, S.D., 1997. Geometric approach to nondestructive identification of faults in stochastic structural systems. *AIAA Journal*, **35**:700-705.
Sakellariou, J.S., Fassois, S.D., 2000. Parametric Output Error Based Identification and Fault Detection in Structures under Earthquake Excitation. European COST F3 Conference on System Identification and Structural Health Monitoring, Madrid, Spain, p.323-332.
Soderstrom, T., Stoica, P., 1989. System Identification. Prentice Hall.
Sohn, H., Farrar, C.R., Hemez, F.M., Shunk, D.D., Stinemates, D.W., Nadler, B.R., 2003. A Review of Structural Health Monitoring Literature: 1996-2001. Los Alamos National Laboratory Report, LA-13976-MS.
Strang, G., 1986. Introduction to Applied Mathematics. Wellsley, Mass., Wellsley-Cambridge Press.
Szaszi, I., Kulcsar, B., Balas, G.J., Bokor, J., 2002. Design of FDI Filter for an Aircraft Control System. Proceeding of American Control Conf., **5**:4232-4237.
Tokatli, F., Cinar, A., Schlesser, J.E., 2005. HACCP with multivariate process monitoring and fault diagnosis techniques: Application to a food pasteurization process. *Food Control*, **16**(5):411-422. [doi:10.1016/j.foodcont.2004.04.008]
Willsky, A.S., 1976. A survey of design methods for failure detection in dynamic system. *Automatica*, **12**(6):601-611. [doi:10.1016/0005-1098(76)90041-8]
Zimmerman, D.C., Lyde, T.L., 1993. Sensor failure detection and isolation in flexible structure using system realization redundancy. *AIAA Journal of Guidance, Control, and Dynamics*, **16**:490-497.